

Transition to a cubic phase with symmetry-breaking disorder in $\text{PbZr}_{0.52}\text{Ti}_{0.48}\text{O}_3$ at high pressure

J. Rouquette, J. Haines,* V. Bornand, M. Pintard, and Ph. Papet

Laboratoire de Physico-Chimie de la Matière Condensée, UMR CNRS 5617, Université Montpellier II Sciences et Techniques du Languedoc, cc 003, Place Eugène Bataillon, 34095 Montpellier cedex 5, France

R. Astier

Institut Gerhardt, Université Montpellier II Sciences et Techniques du Languedoc, cc 003, Place Eugène Bataillon, 34095 Montpellier cedex 5, France

J. M. Léger

Laboratoire des Propriétés Mécaniques et Thermodynamiques des Matériaux, UPR CNRS 9001, Université Paris-Nord, Avenue J. B. Clément, 93430 Villetaneuse, France

F. Gorelli

LENS and INFN, 50019 Sesto Fiorentino (Florence), Italy

(Received 31 January 2002; revised manuscript received 18 March 2002; published 20 May 2002)

The tetragonal perovskite lead zirconate titanate $\text{PbZr}_{0.52}\text{Ti}_{0.48}\text{O}_3$ (PZT), which is an important piezoelectric ceramic material, was found to undergo a phase transition to a cubic phase at close to 5 GPa by x-ray diffraction and Raman spectroscopy. Whereas the x-ray diffraction data indicated no deviation from cubic symmetry above this pressure, a strong Raman signal was present in this phase. The Raman spectrum obtained indicates the presence of symmetry-breaking disorder and is similar to those observed for ferroelectric relaxors. This result is in sharp contrast with the forbidden first-order Raman spectrum, which would be expected for a cubic paraelectric phase such as that observed at high temperature in this material.

DOI: 10.1103/PhysRevB.65.214102

PACS number(s): 77.84.Dy, 62.50.+p, 78.30.-j, 61.50.Ks

I. INTRODUCTION

The perovskite solid solution between lead zirconate and lead titanate $\text{PbZr}_{(1-x)}\text{Ti}_x\text{O}_3$ (PZT) is of great interest due to its very high piezoelectric response near what is termed the “morphotropic phase boundary”¹ between ferroelectric rhombohedral (space group $R3m$) and tetragonal (space group $P4mm$) phases with x values of close to 0.48. Recently, it has been shown that there is in fact a monoclinic phase (space group Cm) (Refs. 2–5) at this region in the phase diagram and that the polar axis in this phase can lie anywhere between the pseudocubic [111] and [001] directions, thus providing a possible origin for this high piezoelectric response. At temperatures close to 650 K depending on the exact composition a transformation to the cubic paraelectric phase (space group $Pm\bar{3}m$) is observed.¹ The dielectric and piezoelectric properties of PZT ceramics, which are mainly governed by domain wall motion, are known to be sensitive to stress induced by external elastic or electric fields,^{6–11} and in this respect it is also very important to understand the effect of hydrostatic pressure on the phase diagram of this material. Our experiments conducted on PZT powder show that the ferroelectric tetragonal phase undergoes a transition to a cubic phase at high pressure; however, the Raman intensity does not disappear as would be expected for a transition to the paraelectric phase and the strong Raman spectrum present for this cubic phase is similar to those observed for ferroelectric relaxors.

II. EXPERIMENT

$\text{PbZr}_{0.52}\text{Ti}_{0.48}\text{O}_3$ was prepared by a conventional solid-state reaction from high-purity (>99.9%) oxides via a two-stage calcination process. To ensure a better distribution of the B-site cations and limit the formation of parasitic pyrochlore-type phases, ZrO_2 and TiO_2 were first ball milled for 4 h in a de-ionized water medium. The slurry was dried and calcined at 1673 K for 4 h to form the corresponding $\text{Zr}_{0.52}\text{Ti}_{0.48}\text{O}_2$ mixed oxide. Stoichiometric amounts of lead oxide were added. The fine-grained (<3 μm) mixtures obtained by attrition milling for 4 h were then calcined in air at 1003 K for 4 h in covered Al_2O_3 crucibles to produce perovskite-type materials. To complete the synthesis, as-obtained powders were pressed to form pellets, fired in a PbO-rich environment at 1523 K and ground leading to high-purity, fine-grained powders. The net weight loss during sintering was limited to 1.3%, which can be correlated¹² to a lead vacancy content of approximately 0.3%. The cell constants of the tetragonal form prepared in this way are $a = 4.0395(5)$ Å and $c = 4.1355(7)$ Å based on data from a θ - 2θ diffractometer using $\text{Cu } K\alpha_1$ radiation.

Angle-dispersive x-ray diffraction data at high pressure were obtained using a diamond anvil cell (DAC). The PZT powder was placed in the 150- μm -diam hole which had been drilled in a stainless-steel gasket preindented to a thickness of 100 μm . Powdered ruby or NaCl were added as pressure calibrants. Pressures were measured based on the shifts of the ruby R_1 and R_2 fluorescence lines¹³ or estimated using the Decker equation of state of NaCl (Ref. 14) with the fol-

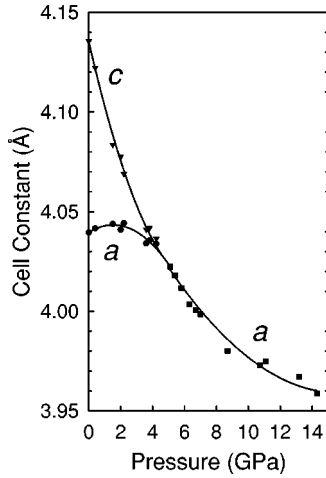


FIG. 1. Cell constants of $\text{PbZr}_{0.52}\text{Ti}_{0.48}\text{O}_3$ as a function of pressure.

lowing bulk modulus and pressure derivatives $B_0 = 23.635$ GPa, $B'_0 = 4.918$, and $B''_0 = -0.0025$. The 21:4:1 methanol:ethanol: H_2O (MEW) mixture used as a pressure-transmitting medium was hydrostatic up to 10 GPa and remained quasihydrostatic up to 15 GPa. X-ray diffraction patterns were obtained with Zr-filtered Mo radiation from an 800-W microfocus tube. X-ray capillary optics were used, giving a 100- μm -diam beam. Detection was performed with an imaging plate placed at 143.61 mm from the sample. Exposure times were typically between 48 and 60 h. The observed intensities on the imaging plates were integrated as a function of 2θ in order to give conventional, one-dimensional diffraction profiles. Rietveld refinements were performed using the program FULLPROF.¹⁵ As the x-ray diffraction from PZT is strongly dominated by scattering from the lead ions, which lie on special positions with no refinable fractional atomic coordinates, these refinements were uniquely used to obtain accurate unit-cell constants. All figures in parentheses refer to estimated standard deviations.

High-pressure Raman experiments were performed using a membrane-type DAC. Samples were loaded along with a ruby crystal using argon or the above MEW mixture as pressure transmitting media in the 150- μm -diam holes of a stainless-steel gaskets, which had been reindented to a thickness of about 50 μm . Raman experiments were performed in a modified backscattering geometry using a Jobin Yvon model U 1000 double monochromator and a liquid-nitrogen-cooled charge-coupled-device (CCD) camera. The 647.1-nm line of a krypton ion laser was used for excitation and the incident laser beam was brought in at an angle of about 15° with respect to the axis of the DAC.

III. RESULTS AND DISCUSSION

The unit-cell constants obtained for the tetragonal phase at ambient pressure are in good agreement with previous work^{2,3,16,17} for $x=0.48$. Compression principally occurs along c , Fig. 1. The a cell constant increases initially with pressure and then decreases. This compression behavior is very similar to what has been previously observed¹⁸ for the

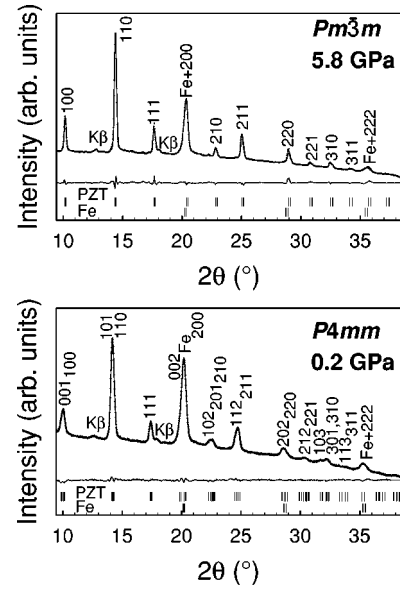


FIG. 2. Experimental (●) and calculated (solid line) diffraction profiles for the tetragonal $P4mm$ [$P=0.2$ GPa, $a=4.0416(3)$ Å, $c=4.1221(5)$ Å] and cubic $Pm\bar{3}m$ [$P=5.8$ GPa, $a=4.0116(1)$ Å] phases of $\text{PbZr}_{0.52}\text{Ti}_{0.48}\text{O}_3$. Vertical bars indicate the calculated positions ($K\alpha_1$ and $K\alpha_2$) of the lines from PZT (upper) and iron (Fe) from the stainless-steel gasket (lower). The strongest $K\beta$ lines are indicated. The principal diffraction lines are indexed and the difference profile is plotted on the same scale. Agreement factors are $R_p=8.8\%$, $R_{wp}=5.6\%$, and $R_{Bragg}=4.6\%$ for the tetragonal phase and $R_p=11.7\%$, $R_{wp}=8.4\%$, and $R_{Bragg}=4.7\%$ for the cubic phase. Note the splitting of the cubic 310 reflection into the 103, 301, and 310 reflections in the tetragonal phase.

tetragonal phase of PbTiO_3 . Above 5 GPa, a transition to the cubic phase occurs as indicated by Rietveld refinements, Fig. 2. Lines which were split in the tetragonal phase have the same linewidth as those that do not split. No deviation from cubic symmetry was observed up to the highest pressure reached. The observed transition pressure is significantly lower than that for the pure end member PbTiO_3 , for which the transition occurs at 12.1 GPa (Ref. 19). The present result for $\text{PbZr}_{0.52}\text{Ti}_{0.48}\text{O}_3$ is also lower than the 8 GPa obtained by linear extrapolation of the dT/dP slope of the tetragonal-cubic phase boundary determined from combined high-pressure, high-temperature dielectric measurements^{20,21} up to 0.8 GPa. However, this linear extrapolation represents a maximum value as close inspection of the dielectric results indicates a tendency towards an increase in the rate of decrease of the critical temperature dT_c/dP with increasing pressure.

The Raman spectrum of $\text{PbZr}_{0.52}\text{Ti}_{0.48}\text{O}_3$, Fig. 3, contains a series of broad overlapping bands and is typical of samples of the tetragonal phase in this composition range. Each band is known to be composed of a series of subpeaks.^{22,23} Strong mode softening is not observed in contrast to the behavior¹⁹ prior to the high-pressure, ferroelectric-paraelectric transition in PbTiO_3 . The broadbands instead have a tendency to harden with increasing pressure with the exception of the mode at just below 210 cm^{-1} , which softens slightly. An increase in intensity at close to 240 cm^{-1} is observed as a

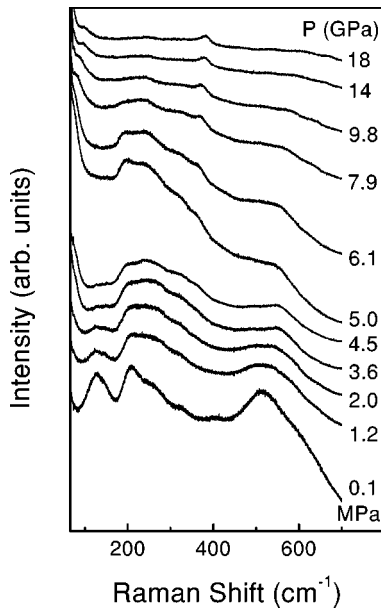


FIG. 3. Raman spectra obtained on decompression from 18 GPa for $\text{PbZr}_{0.52}\text{Ti}_{0.48}\text{O}_3$. Decompression data are presented as they correspond to data obtained for the same quantity of sample as there is no variation in sample thickness in contrast to compression data. The spectra obtained on compression are equivalent; however, there was a decrease in overall intensity with increasing pressure. The ambient data (not to scale) correspond to a fresh powder sample.

function of pressure. This corresponds to a strong band in the rhombohedral and the recently discovered monoclinic phases indicating that domains polarized along the pseudocubic [111] direction may be present. This could also be indicative of a slight monoclinic distortion of the cell or local polar configurations similar to those existing in the monoclinic or rhombohedral phases. A relative decrease in the intensities of the modes in the $450\text{--}650\text{ cm}^{-1}$ region is also observed. The most striking intensity changes are, however, those which are observed for the modes in the region between 125 and 145 cm^{-1} . These modes rapidly decrease in intensity as a function of pressure and disappear at the phase transition pressure. The same behavior has also been observed as a function of temperature.²² In contrast to the high-temperature behavior of PZT, the higher-frequency modes do not decrease in intensity by an order of magnitude at the transition to the cubic phase, but instead retain essentially the same intensity as they had immediately prior to the phase transition. Group theory indicates that the cubic paraelectric phase has no first-order Raman spectrum and, in the case of PbTiO_3 , the first-order Raman spectrum disappears at the tetragonal to cubic transition both at high temperature^{24,25} and high pressure.¹⁹ Weak Raman spectra have been observed for the cubic phases of several perovskites^{26–28} including BaTiO_3 and have been attributed to cation disorder, which induces a loss of the inversion center in the structure and the observation of weak features in the Raman spectrum corresponding to the infrared-active T_{1u} modes and silent T_{2u} mode. The high-pressure cubic phase of PZT, however, exhibits a strong Raman spectrum, which is very similar to those observed for ferroelectric relaxors,^{29–33} such as lanthanum-doped PZT

(PLZT). These spectra are intense due to the existence of randomly oriented polar nanoregions, which arise from symmetry breaking defects.^{34–36} In addition, two new peaks are observed at close to 80 and 360 cm^{-1} . Similar peaks are present in the spectra of the relaxor phases of $\text{PbSc}_{1/2}\text{Ta}_{1/2}\text{O}_3$ (PST) and $\text{PbMg}_{1/3}\text{Nb}_{2/3}\text{O}_3$ (PMN) and were attributed to the E_g and T_{2g} modes from a proposed $Fm\bar{3}m$ supercell³⁷ with $Z=8$. The observed spectrum for the cubic phase of PZT weakens with further increases in pressure due to the gradual reduction in polar domains.

High-pressure, ferroelectric-to-relaxor transitions have been observed in more complex systems,^{38–41} but there have been no reports of such behavior in PZT. In the case of PLZT,^{38,39} there is a transition from the relaxor phase to a normal ferroelectric phase with decreasing temperature, which crosses over to the relaxor phase at high pressure. This process involves a change from long-range order in the ferroelectric phase to short-range order in the relaxor phase. It was found in dielectric studies^{38,39} of PLZT systems up to 2 GPa that high pressure acted in a similar way as increasing La concentration.

The similarity between the spectra obtained for the cubic phase of PZT and those of ferroelectric relaxors raises the question as to the nature of this high-pressure phase. At the present time, it is not yet clear whether the symmetry-breaking disorder is due to off-center shifts of the lead ions as is found in the low-pressure, rhombohedral, monoclinic, and tetragonal ferroelectric phases^{17,42} or to differences in the local environments around the B cations (ABO_3 : $A=\text{Pb}$, $B=\text{Ti,Zr}$) or a combination of both effects. It can be noted that neutron diffraction results indicate that for the ferroelectric phases, the z coordinates of Ti^{4+} and Zr^{4+} , which are not the same size, are generally different.^{17,42} It is well known that, in particular, Ti^{4+} is more polarizable than Zr^{4+} and often adopts rather distorted off-center octahedral coordination.^{43,44} Disorder induced by the small amount of vacancies on the Pb^{2+} sites may also play a role. These are all sources of local polarization in the cubic phase, and the length scale of these phenomena remains to be determined.

IV. CONCLUSIONS

The present x-ray diffraction and Raman scattering results on $\text{PbZr}_{0.52}\text{Ti}_{0.48}\text{O}_3$ at high pressure provide evidence for a novel phase transition in this system. The tetragonal-to-cubic phase transition occurs at 5 GPa; however, a strong Raman spectrum is also observed in the cubic phase. This spectrum indicates the presence of symmetry-breaking disorder and is similar to those observed in relaxor systems. This phase is distinct from the high-temperature paraelectric phase, which has only a weak Raman spectrum.

ACKNOWLEDGMENTS

We would like to thank the European Union for funding the work at LENS under Contract No. HPRICT 1999-00111 and R. Bini, L. Ulivi, and M. Santoro for useful discussions.

- *Corresponding author. Electronic address: jhaines@lpmc.univ-montp2.fr
- ¹B. Jaffe, W. R. Cook, and H. Jaffe, *Piezoelectric Ceramics* (Academic, London, 1971).
 - ²B. Noheda, D. E. Cox, G. Shirane, J. A. Gonzalo, L. E. Cross, and S.-E. Park, *Appl. Phys. Lett.* **74**, 2059 (1999).
 - ³B. Noheda, J. A. Gonzalo, L. E. Cross, R. Guo, S.-E. Park, D. E. Cox, and G. Shirane, *Phys. Rev. B* **61**, 8687 (2000).
 - ⁴R. Guo, L. E. Cross, S.-E. Park, B. Noheda, D. E. Cox, and G. Shirane, *Phys. Rev. Lett.* **84**, 5423 (2000).
 - ⁵B. Noheda, D. E. Cox, G. Shirane, R. Guo, B. Jones, and L. E. Cross, *Phys. Rev. B* **63**, 014103 (2000).
 - ⁶D. Damjanovic, *J. Appl. Phys.* **82**, 1788 (1997).
 - ⁷Q. M. Zhang, J. Zhao, K. Uchino, and J. Zheng, *J. Mater. Res.* **12**, 226 (1997).
 - ⁸D. Audigier, Cl. Richard, Cl. Deschamps, M. Troccaz, and L. Eyraud, *Ferroelectrics* **154**, 219–224 (1994).
 - ⁹W. R. Biessem, L. E. Cross, and A. K. Goswami, *J. Am. Ceram. Soc.* **1**, 36 (1966).
 - ¹⁰Q. M. Zhang and Z. Jianzhong, *IEEE Trans. Ultrason. Ferroelectr. Freq. Control* **46**, 1518 (1999).
 - ¹¹N. J. Ramer, S. P. Lewis, E. J. Mele, and A. M. Rappe, in *First-Principles Calculations for Ferroelectrics*, edited by Ronald E. Cohen, AIP Conf. Proc. No. 436 (AIP, Woodbury, NY, 1998), p. 156.
 - ¹²F. Chu, I. M. Reaney, and N. Setter, *J. Appl. Phys.* **77**, 1671 (1995).
 - ¹³H. K. Mao, J. Xu, and P. M. Bell, *J. Geophys. Res.* **91**, 4673 (1986).
 - ¹⁴D. L. Decker, *J. Appl. Phys.* **42**, 3239 (1971).
 - ¹⁵J. Rodríguez-Carvajal (unpublished).
 - ¹⁶M. R. Soares, A. M. R. Senos, and P. Q. Mantas, *J. Eur. Ceram. Soc.* **20**, 321 (2000).
 - ¹⁷J. Frantti, J. Lappalainen, S. Eriksson, V. Lantto, S. Nishio, M. Kakihana, S. Ivanov, and H. Rundlof, *Jpn. J. Appl. Phys., Part 1* **39**, 5697 (2000).
 - ¹⁸R. J. Nelmes and A. Katrusiak, *J. Phys. C* **19**, L725 (1986).
 - ¹⁹J. A. Sanjurjo, E. López-Cruz, and G. Burns, *Phys. Rev. B* **28**, 7260 (1983).
 - ²⁰M. Pisarski, *Ferroelectrics* **81**, 297 (1988).
 - ²¹M. Pisarski, *Ferroelectrics* **94**, 215 (1989).
 - ²²J. Frantti and V. Lantto, *Phys. Rev. B* **56**, 221 (1997).
 - ²³K. C. V. Lima, A. G. Souza Filho, A. P. Ayala, J. Mendes Filho, P. T. C. Freire, and F. E. A. Melo, *Phys. Rev. B* **63**, 184105 (2001).
 - ²⁴G. Burns and B. A. Scott, *Phys. Rev. Lett.* **25**, 167 (1970).
 - ²⁵G. Burns and B. A. Scott, *Phys. Rev. B* **7**, 3088 (1973).
 - ²⁶M. D. Fontana and M. Lambert, *Solid State Commun.* **10**, 1 (1972).
 - ²⁷A. K. Sood, N. Chandrabhas, D. V. S. Muthu, and A. Jayaraman, in *Proceedings of the XIVth International Conference on Raman Spectroscopy, Hong Kong, 1994*, edited by N. T. Yu and X. Y. Li (Wiley, New York, 1994), p. 1048.
 - ²⁸D. Gourdain, E. Moya, J. C. Chervin, B. Canny, and Ph. Pruzan, *Phys. Rev. B* **52**, 3108 (1995).
 - ²⁹I. G. Siny and T. A. Smirnova, *Ferroelectrics* **90**, 191 (1989).
 - ³⁰M. El Marssi, R. Farhi, X. Dai, A. Morell, and D. Viehland, *J. Appl. Phys.* **80**, 1079 (1996).
 - ³¹I. G. Siny and R. S. Katiyar, *Ferroelectrics* **223**, 35 (1999).
 - ³²I. G. Siny, E. Husson, J. M. Beny, S. G. Lushnikov, E. A. Rogacheva, and P. P. Syrnikov, *Ferroelectrics* **248**, 57 (2000).
 - ³³J. Kreisel, A. M. Glazer, P. Bouvier, and G. Lucazeau, *Phys. Rev. B* **63**, 174106 (2001).
 - ³⁴H. Uwe, K. B. Lyons, H. L. Carter, and P. A. Fleury, *Phys. Rev. B* **33**, 6436 (1986).
 - ³⁵P. DiAntonio, B. E. Vugmeister, J. Toulouse, and L. A. Boatner, *Phys. Rev. B* **47**, 5629 (1993).
 - ³⁶J. Toulouse, P. DiAntonio, B. E. Vugmeister, X. M. Wang, and L. A. Knauss, *Phys. Rev. Lett.* **68**, 232 (1992).
 - ³⁷I. G. Siny and C. Boulesteix, *Ferroelectrics* **96**, 119 (1989).
 - ³⁸G. A. Samara, *Phys. Rev. Lett.* **77**, 314 (1996).
 - ³⁹G. A. Samara, *J. Appl. Phys.* **84**, 2538 (1998).
 - ⁴⁰G. A. Samara and L. A. Boatner, *Phys. Rev. B* **61**, 3889 (2000).
 - ⁴¹G. A. Samara, E. L. Venturi, and V. H. Schmidt, *Phys. Rev. B* **63**, 184108 (2001).
 - ⁴²D. L. Corker, A. M. Glazer, R. W. Whatmore, A. Stallard, and F. Fauth, *J. Phys.: Condens. Matter* **10**, 6251 (1998).
 - ⁴³M. Kunz and I. D. Brown, *J. Solid State Chem.* **115**, 395 (1995).
 - ⁴⁴J. Frantti, J. Lappalainen, V. Lantto, S. Nishio, and M. Kakihana, *Jpn. J. Appl. Phys., Part 1* **39**, 5679 (2000).